PROCEEDINGS, 51st Workshop on Geothermal Reservoir Engineering
Stanford University, Stanford, California, February 9-11, 2026
SGP-TR-230

The Evolution of Well 58-32 at Utah FORGE in Response to Fluid Flow Along a Stimulated Fracture Corridor

Stuart F. Simmons[1], Clay Jones[1], Tobias Fischer[2], Paul von Hirtz[3], Peter Meier[4] and Joe Moore[1]

[1]EGI, University of Utah, Salt Lake City, UT 84108, USA
[2]Department of Earth Science, University of California Santa Barbara, Santa Barbara, CA 93106-9630, USA
[3]Thermochem, 3414 Regional Parkway, Santa Rosa, CA 95403
[4]Geo-Energie Suisse AG, Reitergasse 11, CH-8004, Zurich, Switzerland

ssimmons@egi.utah.edu

Keywords: geochemistry, stimulation, 58-32, Utah FORGE, enhanced geothermal systems, reservoir monitoring

ABSTRACT

Well 58-32 was completed in September 2017, providing confirmation of a hot dry granitic rock reservoir at drillable depths that advanced development of the Utah FORGE field laboratory. Apart from small scale injection testing in 2019, the well was used for the temporary deployments of geophone strings and seismic monitoring during drilling and stimulation operations related to the completion of wells 16A(78)-32 and 16B(78)-32. In this early phase of EGS reservoir development through to at least 2022, the water levels in 58-32 were relatively static, and the water composition showed a moderate increase in total dissolved salts compared to the culinary grade water with which it was originally filled. Further compositional evolution occurred by 2024, which is believed to be related to stimulation of stage 9 in 16A(78)-32. The associated sharp pressure rise led to removal of geophones, and at the start of the four-week circulation test in August 2024, vigorous gas bubbling was noticed. The well was shut in, and a flow line was added to sample and monitor fluids safely. When subsequently opened for short periods to acquire samples, a frothy two-phase fluid discharged, and chemical analyses indicated the well water had transformed into a carbon dioxide rich saline solution. Furthermore, connection had been made with the Utah FORGE reservoir, 200 m away. Separately, temperature logs show that the conditions remained unchanged from its original conductive gradient. In this report, an overview of changes in 58-32 fluid chemistry, including results of recent downhole sampling, are described. Provisionally, these data provide clues regarding the character of fluids occupying the periphery of stimulated fractures in the Utah FORGE EGS reservoir.

1. INTRODUCTION

Well 58-32 is a vertical well that was completed in September 2017, and it was the first geothermal well drilled in the Milford valley outside of Roosevelt Hot Springs in over 30 years. It provided critical confirmation of conditions favorable to EGS development in a hot dry granitic rock reservoir at Utah FORGE (Allis and Moore, 2019). In the period following its completion, 58-32 has been used primarily for temporary deployments of geophones during stimulation operations of wells 16A(78)-32 and 16B(78)-32 (Figure 1). When 58-32 began flowing during early phases of the April 2024 stimulation program, the geophone strings were pulled, marking what appears to have been transformation of the wellbore fluid. The change in fluid composition was finally quantified with the installation of a flow line in August 2024 that enabled fluid sampling and analysis during the August-September 2024 circulation test. Additional data were obtained during short circulation tests in late June and late August, 2025. At the end of August 2025, a bridge plug was set at 6500 feet depth to isolate and protect future deployments of geophone strings in the overlying interval. Before doing so, however, Thermochem was contracted to obtain and analyze downhole samples of fluid providing deep to shallow chemical characterization of the well bore. The summary of results that follows documents the evolution of fluids in well 58-32 in response to stimulation, pressurization and fluid movement along a stimulated fracture corridor.

2. SHORT HISTORY OF WELL 58-32 (2017-2025)

Well 58-32 was spudded on July 31, 2017, and it was drilled vertically to 7536 ft (2298 m) depth from a surface elevation of 5528 ft (1685 m) above sea level. The well penetrated layered alluvium deposits down to 3176 ft (968 m), where it crossed the contact with underlying crystalline basement rocks, which make up the rest of the stratigraphy to the bottom of the hole (Jones et al., 2019). No loss fluid zones were encountered during drilling reflecting the tight impermeable nature of the basement reservoir rock. The well was plugged back to 7525 ft depth, and 7-inch casing was cemented to 7375 ft depth leaving the bottom open.

Before the rig was released September 24, 2017, the well was flushed and filled with fresh water from Milford, and a final warm up pressure-temperature survey was conducted November 2, 2017, at which time the water level was ~5500 ft above sea level. A second pressure-temperature survey was conducted November 9, 2018, at which time the water level dropped to 5220 ft above sea level. These two logs as well as all subsequent logs produced consistent results, showing a conductive thermal gradient (>70°C/km) and a bottom hole temperature between 195° and 200°C (Allis et al., 2019).

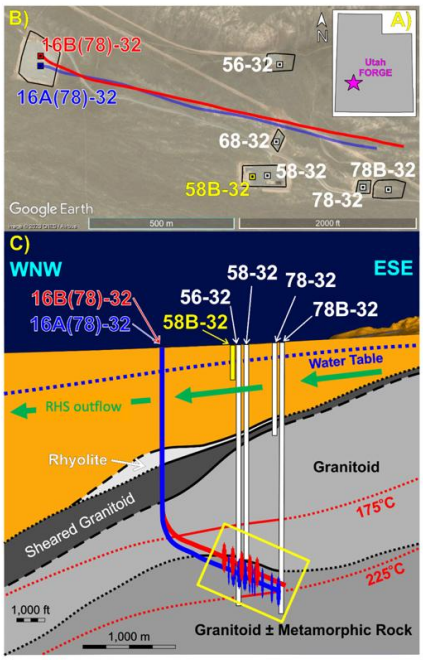

Figure 1. Map (A), plan (B) and cross section (C) views of the location of the Utah FORGE site, wellfield layout and the underlying geology hosting the EGS reservoir outlined in yellow. The reservoir rocks comprise granitoids and gneiss, which are composed mainly of alumino-silicate minerals and quartz (Jones et al., 2024). The green arrows mark the outflow of thermal waters from Roosevelt Hot Springs (RHS), which is pumped from well 58B-32 for water supply during circulation testing.

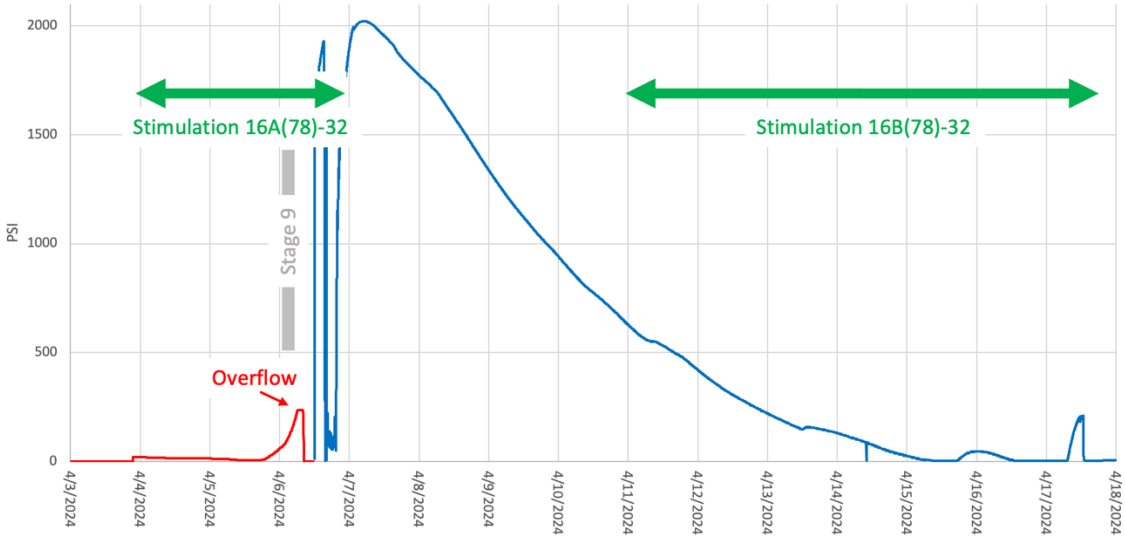

Figure 2. Continuous pressure record of well 58-32 during stimulation testing in April 2024. The red line marks data obtained from a down hole pressure transducer, and the blue represents data from a wellhead gauge. Well 16A(78)-32 was stimulated April 4-7, and well 16B(78)-32 was stimulated April 11-24. The initial pressurization that induced water level rise and overflow correlates with the period of stage 9 stimulation in 16A(78)-32.

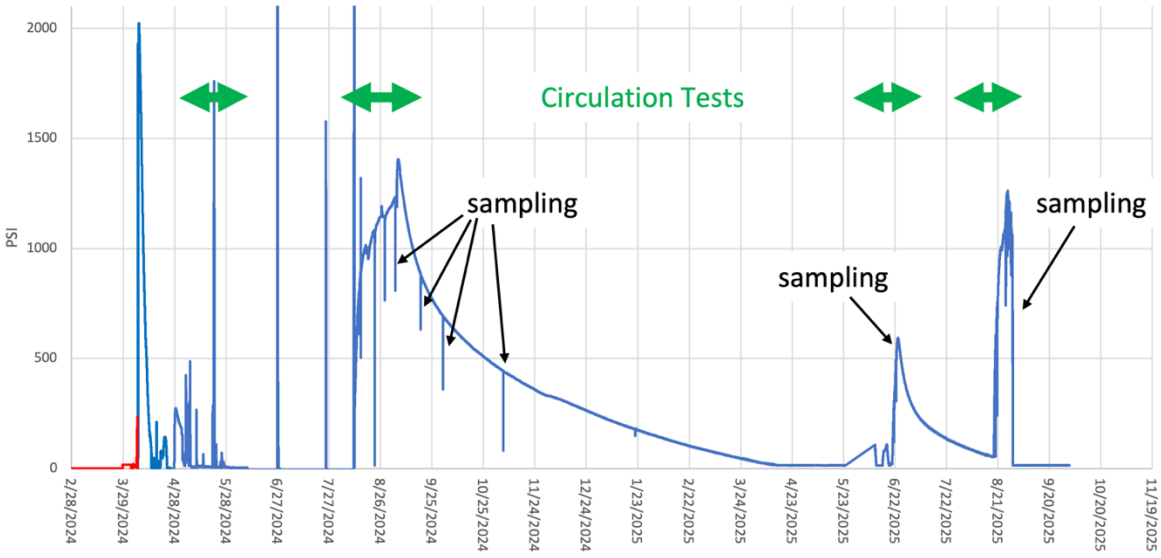

Figure 3: Continuous pressure record of well 58-32 from April 2024 through September 2025, during which four circulation tests were carried out.

Small scale injection tests using fresh water were carried out in 2017 and 2019 in the barefoot interval and up hole in perforated casing between 6955 and 6965 ft depth (Xing et al., 2020); injection of a third shallower perforated interval was attempted but failed despite a wellhead pressure of 6500 psi.

A third pressure-temperature survey was conducted June 28, 2021, indicating a water level of 5036 ft above sea level. In June 2023, installation of a pressure transducer with a temperature sensor was set just below the water level at 4990 ft above sea level providing continuous monitoring for the next two months during which there was minimal fluctuation in recorded data. The drilling of the groundwater supply well 58B-32 nearby in December 2023 indicated a local groundwater elevation of 5040 ft above sea level measured in February 2024.

Continuous pressure monitoring of 58-32 commenced late March 2024 before stimulation testing in wells 16A(78)-32 and 16B-(78)-32 began in early April. The 58-32 water level at that time was 5030 ft above sea level. It remained static until just before the stimulation of stage 9 in well 16A(78)-32, when over a 12-hour period it rose ~500 ft and began overflowing. The temporary geophone string was then pulled, the well was shut in, and the pressure rose sharply peaking at 2000 psi, tailing off over the next few days (Figure 2).

During the stimulation of 16A(78)-32 (April 4-7, 2024), ~118,000 bbl of water total were injected at between 5000 and 8000 psi. In the subsequent stimulation of 16B(78)-32 (April 11-24, 2024), ~17,000 bbl of water total were injected at between 5000 and 8000 psi; this activity induced only small transient pressure perturbations in 58-32 (Figure 2). During the 9-hour circulation test (April 27-28, 2024) that followed, ~6900 bbl of water total were injected into 16A(78)-32 at between 3000 and 3500 psi, with ~2400 bbl of water being produced from 16B(78)-32; this activity induced transient pressurization of 58-32 up to 250 psi (Figure 3).

From August 8 to September 3, 2024, the longest-term circulation test was run during which a total of ~360,000 bbl of water were injected into 16A(78)-32 at 3000 psi and ~239,000 bbl water were produced from 16B(78)-32 at 200 psi. Pressurization of the reservoir again induced a response in 58-32, first with bubbling and exsolution of gas at the wellhead followed by a sharp pressure increase once the well had been shut in (Figures 3 and 4). The installation of a horizontal flow line to the pit allowed for fluid sampling (Table 1), and the results of are described in the next section. The first sampling was carried out on August 22, and subsequent samples were obtained through to November 5. On each occasion, the well discharged a cool (~20° C) frothy white two-phase fluid (Figure 4). Initial flow rates were the strongest, but never particularly energetic, and they declined over the period of sampling usually lasting up to 30-40 minutes. Once completed and the wellhead valve was closed, the pressure quickly rebounded to the pre-sampling level; the fall and rise in pressure during sampling periods are clearly evident as spikes in the time series graph in Figure 3. At the end of the circulation test in early September, wells 16A(78)-32 and 16B(78)-32 were shut in, and the pressure in all three wells, 58-32 inclusive, followed strongly similar trends, declining gradually through to the first quarter of 2025 (Figure 3).

In 2025, two short circulation tests were run. The first in June followed a phase of servicing in which both the injection and production wells were cleaned out. The second in August was run as part of the R&D program. In both periods, pressurization of the reservoir affected 58-32 (Figure 3), during which additional fluid samples were obtained (Table 1). At the end of the field experiments, downhole sampling was performed (August 27-28) after which a bridge plug was cemented into place (August 29).

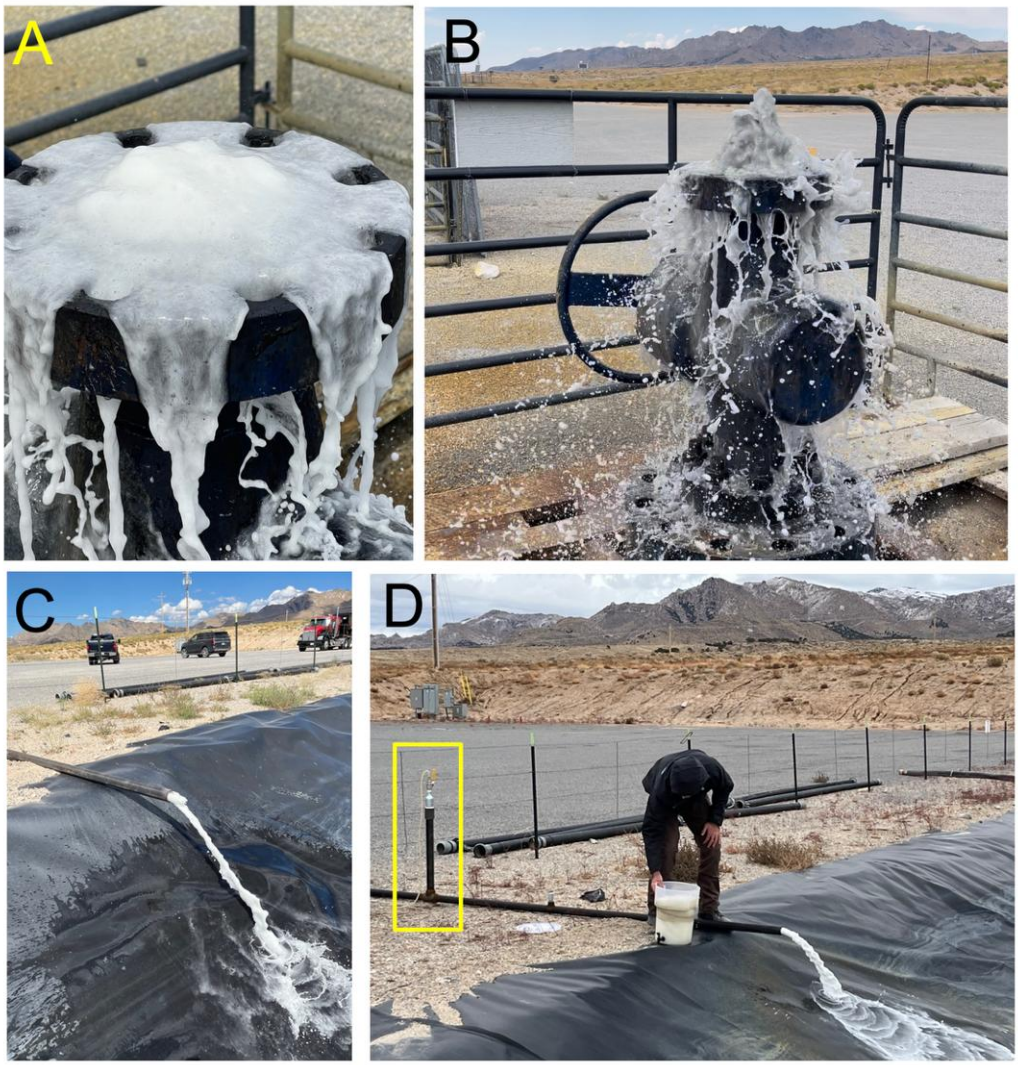

Figure 4: Images of fluid discharge at 58-32: A) and B) represent the first observations of well overflow August 10, 2024; C) and D) represent two-phase flows that were sampled on August 22 and November 5, 2024 from the flow line between the wellhead and the pit. The yellow box in D) highlights the vertical pipe connection from which dry gas samples were obtained.

In summary, the record of sporadic water level measurements and continuous pressure monitoring since late March 2024 show that prior to the April 2024 stimulation campaign, the pressure head on the water filling 58-32 was similar to the local hydrostatic head controlling the aquifer tapped by 58B-32. This appears to have remained unchanged through to the stimulation of stage 9 in well 16A(78)-32, when physical connection between the production-injection well doublet and 58-32 was established. Separately, the volumes of flowback water during the drilling out of the frac plugs in 16A(78)-32 and a spinner injection profile in 16A(78)-32 (August 17, 2024) from the circulation test both showed that stage 9 was interconnected with the previous frac stage 8. This is further supported by the strong clustering of microseismicity along a NNE trending corridor during stimulation and subsequent circulation testing (e.g., Niemz et al., 2025).

3. COMPOSITIONS OF 58-32 BORE WATERS

As indicated, 58-32 was originally designed for reservoir characterization and seismic monitoring. In 2022, the first water sample was obtained using a bailer when the water level was ~500 ft below the surface, and subsequent fluid samples were taken on a regular basis during circulation tests in 2024 and 2025 (Tables 1, 2 and 3). Analytical results were supplied through Thermochem except for the analysis of drinking water from the Milford town supply, which was obtained through the Brigham Young University geochemistry lab (Simmons and Kirby, 2024).

These data raised several questions and concerns about their origins and the potential for casing corrosion. Consequently, Thermochem was contracted to sample and analyze wellbore fluids, using their state-of-the-art downhole sampling tool. This device has a titanium flow-path and inert-gas charged sample chamber which allows for high-accuracy liquid and gas sample recovery from single-phase brine, steam and two-phase wellbore fluids; the tool also captures pressure/temperature/spinner (PTS) log data. Downhole samples were retrieved from depths of 3000 ft (914 m), 6770 ft (2064 m), and 7350 ft (2240 m) below the surface, when the reservoir was pressurized

and the 58-32 wellhead pressure was 1150 psi (7.9 MPa). Vertical profiles of the results are plotted in Figures 6 and 7, and the measurements indicate the bore fluid was well below vapor-gas saturation. Two-phase flow conditions were transient and restricted to the upper most level of the water column during sampling periods when the reservoir was pressurized.

3.1 Evolution of Water Chemistry 2017-2025

Figure 5 shows the evolution of the water chemistry through time. Notable changes include the significant increases in all solutes, a feature that is apparent by 2022 when compared to the fresh water originally filling the well. For example, the chloride concentration increases ten-fold, the bicarbonate concentration nearly doubles, the sulfate decreases to around one fifth, and the pH decreased from 7.8 to 6.5. The origin of the 2022 water remains unclear, but it was distinctly different from water in 58B-32 and from the water that subsequently filled the well in 2024-25 (Table 1).

By 2024, the water composition evolved further becoming more concentrated in most analytes, whereas the sulfate concentration decreased further. The concentrations of chloride, silica, and boron reached ~5500 mg/kg, ~200 mg/kg, and ~35 mg/kg respectively, resembling produced thermal waters from 16B(78)-32 in the same period (Simmons et al., 2025).

The 2025 compositional data are similar, but now having also analyzed iron, anomalously high concentrations (182-294 mg/kg) were measured. Analyses of dry gas samples further revealed the predominance of carbon dioxide and methane in near equal proportion (Table 2), with the concentration of methane being greatly elevated compared to all previous measurements of produced fluids (Simmons et al., 2025). Isotopic analyses of sampled fluids (Table 2) indicate that significant amounts of the carbon and helium are deep sourced, originating in the upper mantle with contributions from the crust.

3.2 Downhole Samples August 27-28, 2025

The analytical results (Tables 1 and 3; Figure 7) indicate chloride is the predominant aqueous species, but with a concentration gradient that gradually decreases upward from 6260 to 5670 mg/kg and closely paralleled by sodium. Dissolved carbon dioxide (less HCO_3) by contrast gradually increases upward from 2950 to 3410 mg/kg, and this gradient may relate to the effect of increasing gas solubility with decreasing temperature. Unfortunately, the concentration of carbon dioxide in the near surface regime is not quantified because only dry gas sampling was possible.

Although unrelated chemically, sulfate and silica have nearly the same concentrations in the deep samples. Upwards, sulfate increases slightly, having a maximum concentration of 314 mg/kg at 914 m depth, but at the surface drops to <1 mg/kg. The silica trend decreases gradually from 284 to 194 mg/kg from bottom to top corresponding to quartz-silica equilibration temperatures from 205 to 178°C. Calcium decreases from 111 to 35.5 mg/kg from bottom to top, whereas iron increases from 6 to >180 mg/kg.

The shallow well water based on sampling of surface discharges is chemically distinct with depleted sulfate and greatly elevated iron. Additionally, the surface dry gas samples contain similar proportions of carbon dioxide and methane, the latter being anomalously enriched compared to gas compositions deeper in the well and to fluids produced from 16B(78)-32. These data indicate methane is sourced in situ from shallow level in the well. Furthermore, the elevated iron and dissolved hydrogen at 914 m in 58-32 suggest the upper casing is being corroded in a strongly reducing environment that partially converts carbon dioxide to methane. A casing survey performed just prior to the downhole sampling, however, indicates that any possible impacts or degradation to well integrity are imperceptible.

Speciation calculations indicate that deep (2064 and 2240 m) well waters are supersaturated in Mg-silicates, carbonate minerals (calcite, dolomite), anhydrite and quartz at 186 to 198°C whereas at 914 m the well water is supersaturated in siderite and quartz at 100°C. At the time of downhole sampling, no restrictions were encountered, and evidence of mineral deposition was not detected.

Table 1: Partial chemical analyses of 58-32 well waters, compared to Milford and 58B-32 waters; concentrations in mg/kg.

		pH	Na	Ca	Cl	B	SiO_2	SO_4	HCO_3	Fe
Milford	7/11/18	7.8	59	12	67	0.1	28	93	140	0.02
58B-32 2024	2/21/24	7.21	1435	198	2715	22.60	66	99	314	0.42
58-32 Surface										
bailer	6/15/22	6.49	214	94.3	509	1.7	10.9	19.9	273	na
well flow line	8/22/24	6.38	3550	94.6	5460	36.5	205	4.57	1200	na
well flow line	9/3/24	6.40	3580	66.5	5520	35.8	208	0.4	1190	na
well flow line	6/22/25	6.28	3530	65.1	5520	36.8	126	6.19	1250	192
well flow line	8/19/25	6.27	3560	51.8	5480	37.6	181	1.52	1260	284
well flow line	8/20/25	6.27	3570	35.5	5490	37.3	194	0.167	1000	182
58-32 Downhole										
914 m (100°C)	8/27/25	6.18	3650	45.1	5670	38.3	280	314	430	54
2064 m (186°C)	8/28/25	6.36	3880	105	6260	29.6	276	296	408	8
2240 m (196°C)	8/28/25	6.43	3900	111	6260	27	284	274	407	6

Table 2: Chemical analyses of dry gas samples collected at the surface from 58-32. Gas concentrations are reported in wt. %, carbon isotope ratios in per mil units, and helium isotope ratios as R/Ra values.

Single Phase Dry Gas		CO_2	H_2S	NH_3	Ar	N_2	CH_4	H_2	$\delta^{13}CO2$	$\delta^{13}CH4$	R/Ra
	8/19/25	56.9	<.00237	0.003	0.005	6.7	36.3	<0.115	-4.19 to -4.23	-55.8 to -58.1	2.05
	8/20/25	45.2	<.00238	<.0113	0.006	8.0	46.7	<0.113	-4.83 to -4.99	-59.0 to -59.4	2.05

Table 3: Chemical analyses of gaseous species in 58-32 downhole water samples; concentrations in mg/kg.

	depth ft	depth m	CO_2	H_2S	NH_3	Ar	N_2	CH_4	H_2	brine
8/27/25	3000	914	3410	1.02	4.18	0.9850	87.3	4.66	46.9	996445
8/28/25	6770	2064	3050	2.23	2.96	0.5530	68.8	2.61	<1.79	996873
8/28/25	7350	2240	2950	3.6	2.94	0.8260	<101	2.52	<1.96	997040

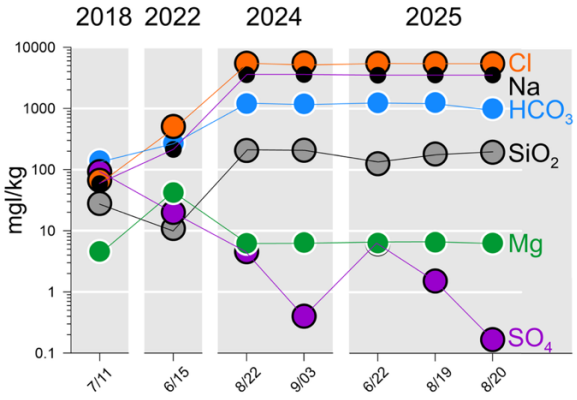

Figure 5: Changes in 58-32 water chemistry through time.

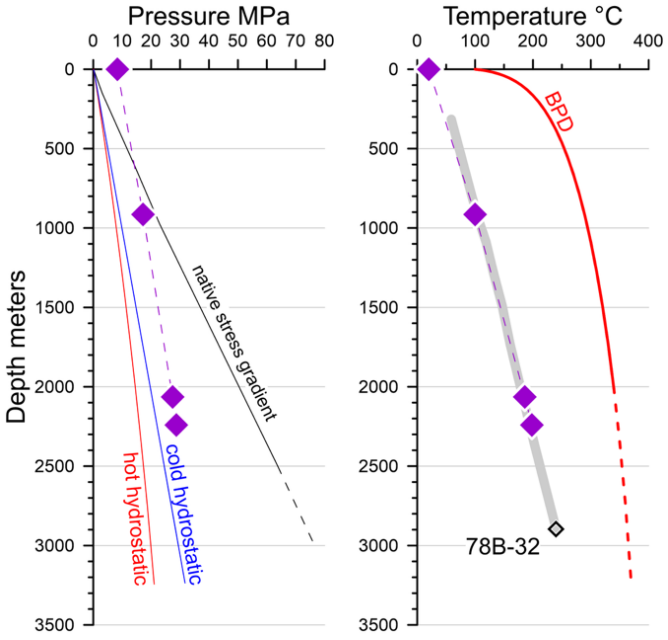

Figure 6. Pressure and temperature gradients measured in well 58-32, August 27-28, 2025 shown in purple filled diamonds. The native stress and hydrostatic gradients, along with the boiling point for depth curve (BPD) and 78B-32 temperature gradient in light grey, are shown for comparison.

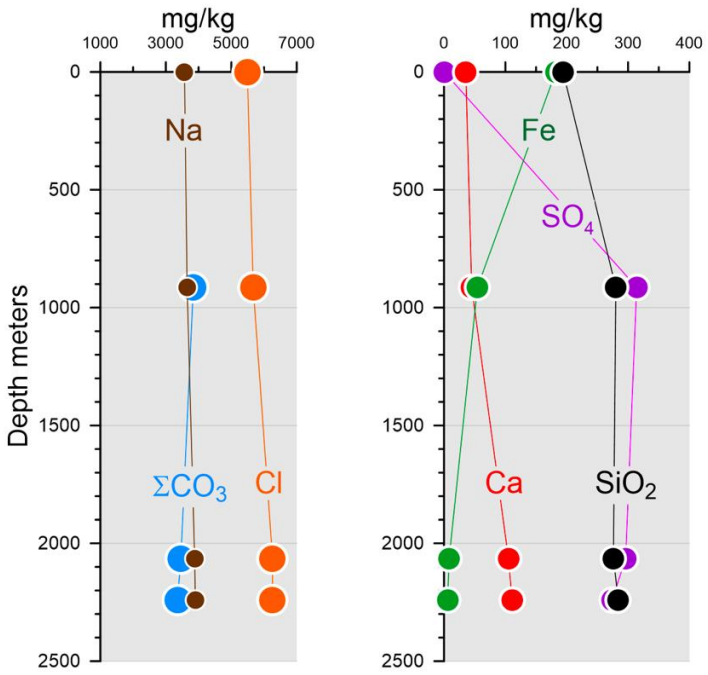

Figure 7. Vertical profiles of chemical data in well 58-32, August 27-28, 2025.

4. SUMMARY OF KEY RESULTS

The compositions of 58-32 evolved from fresh water to a carbonic brine over time. Between 2017 and 2022, this evolution resulted in a three-fold increase in total dissolved solutes. In 2024 and 2025, an additional ten-fold increase in total dissolved solutes occurred, which is believed to correlate with reservoir stimulation that established a fluid flow connection between 58-32 and the injection-production well doublet comprising 16A(78)-32 and 16B(78)-32. This flow connection appears to be localized on a sub-vertical NNE-SSW trending fracture network based on the narrow clustering of stimulation induced microseismicity (Niemz et al., 2025). The sharp rises in pressure associated with short circulation tests in 2025 shows that the connection has been sustained through a relatively long intervening period of reservoir depressurization.

The pressure and temperature profiles obtained during downhole sampling indicate fluid filling the well was a single-phase liquid. The analyses of waters revealed seemingly minor compositional differences from intermediate to deep level. The deepest water has the highest concentrations of chloride, sodium, calcium, and silica; these solutes decrease in concentration upward. Other solutes, including aqueous carbon dioxide, sulfate and iron, show the opposite trend and rise slightly in concentration upwards. All three downhole samples have silica concentrations that correlate with a quartz equilibria temperature ~205°C consistent with measured temperature deep in the well. However, for the sample taken at 3000 ft (914 m) depth, the quartz equilibria temperature is >100°C hotter than the measured temperature of 100°C.

The composition of well waters discharged at the surface are strikingly different having strongly elevated methane and iron, and depleted sulfate, which suggest that reaction with the well casing induced methane formation and chemical reduction. Although there appears to have been no degradation to integrity of the well, carbonic waters are known to be highly corrosive and capable of damaging effects (e.g. Zarrouk, 2004; Arikan et al. 2025). The differences in deep versus shallow water chemistry also has consequences for interpretation of reservoir processes, and the deep-water data are currently believed to better reflect the composition of fluid occupying the host rocks in the vicinity of the well.

Although evidence of mineral deposition was not detected, speciation calculations indicate that well waters are supersaturated in several mineral phases (i.e., Mg-silicates, carbonate minerals, anhydrite, and quartz).

Fluid egress most likely occurred through the uncased and perforated intervals at the bottom of 58-32. The sharp decreases in pressure and in the flow rate of wellhead discharge during fluid sampling (Figure 3) indicate that deep flow into the well is impeded, perhaps by some combination of distance from wells 16A(78)-32 and 16B(78)-32, narrowing fracture apertures, and frictional effects. There is no indication of any accompanying heat transfer.

Given the offset position of well 58-32, the data provide direct measurement of fluid conditions and reservoir characteristics on the periphery of stimulated fractures at Utah FORGE.

5. ACKNOWLEDGEMENTS

Funding for this work was provided by U.S. Department of Energy under grant DE-EE0007080 “Enhanced Geothermal System Concept Testing and Development at the Milford City, Utah FORGE Site”. Thanks are extended to the Utah Geological Survey, the Utah Trust Lands Administration, and Beaver County for their additional support.

REFERENCES

Allis, R., and Moore, J.N., editors, Geothermal Characteristics of the Roosevelt Hot Springs System and Adjacent FORGE EGS Site, Milford Utah, Utah Geological Survey Miscellaneous Publication, 169**,** (2019).

Allis, R., Gwynn, M., Hardwick, C., Hurlbut, W., Kirby, S., and Moore, J.N.: Thermal characteristics of the Roosevelt Hot Springs system, with focus on the FORGE EGS site, Milford, Utah, Utah Geological Survey Miscellaneous Publication 169-D (2019).

Arikan, E., Meyram, M., and Aydin, H.: Casing collapse mechanism in geothermal drilling in western Turkey, 50th Workshop on Geothermal Reservoir Engineering, Stanford University, Stanford, CA (2025).

England, K., Swearingen, L., and McLennan, J.: Extended Circulation Test Report Utah FORGE 16A(78)-32 and 16B(78)-32, EGI, University of Utah, (2024), Geothermal Data Repository, https://doi.org/10.15121/2475065.

Jones, C.G., Moore, J.N., and Simmons, S.: Petrography of the Utah FORGE site and environs, Beaver County, Utah, *in* Allis, R., and Moore, J.N., editors, Geothermal characteristics of the Roosevelt Hot Springs system and adjacent FORGE EGS site, Milford, Utah, Utah Geological Survey Miscellaneous Publication 169-K, **(**2019).

Jones, C. G., Simmons, S., and Moore, J.: Geology of the Utah Frontier Observatory for Research in Geothermal Energy (FORGE) Enhanced Geothermal System (EGS) site, Geothermics, 122, (2024), https://doi.org/10.1016/j.geothermics.2024.103054.

Niemz, P., Pankow, K., Isken, M.P., Whidden, K., McLennan, J. and Moore, J.: Mapping fracture zones with nodal geophone patches: insights from induced microseismicity during the 2024 stimulations at Utah FORGE, Seismological Research Letters 96 (3), (2025) 1603–1618.

Simmons, S. F. and Kirby, S.: Formation of a large cold groundwater mantle helium anomaly and high temperature geothermal resources in response to bimodal magmatism near Roosevelt Hot Springs and Utah FORGE, Milford valley, southwest Utah, Geochemistry, Geophysics, Geosystems 25 (2024).

Simmons, S. F., Jones, C. G., Rose, P., and Moore, J.: The geochemistry of flowback and produced waters at Utah FORGE and their implications for EGS production, 50th Workshop on Geothermal Reservoir Engineering, Stanford University, Stanford, CA (2025).

Xing, P., Moore, J., and McLennan, J.: In-Situ Stress Measurements at the Utah Frontier Observatory for Research in Geothermal Energy (FORGE) Site, Energies, 13 (21), (2020).

Zarrouk, S.J.,: External casing corrosion in New Zealand Geothermal Wells, 26th New Zealand Geothermal Workshop, (2004), 75-81.

.